CELLULAR NEUROSCIENCE

Inflammation up-regulates cochlear expression of TRPV1 to potentiate drug-induced hearing loss

Meiyan Jiang[1]*, Hongzhe Li[1]*†, Anastasiya Johnson[1], Takatoshi Karasawa[1], Yuan Zhang[1], William B. Meier[1], Farshid Taghizadeh[1], Allan Kachelmeier[1], Peter S. Steyger[1,2‡§]

Aminoglycoside antibiotics are essential for treating life-threatening bacterial infections, despite the risk of lifelong hearing loss. Infections induce inflammation and up-regulate expression of candidate aminoglycoside-permeant cation channels, including transient receptor potential vanilloid-1 (TRPV1). Heterologous expression of TRPV1 facilitated cellular uptake of (fluorescently tagged) gentamicin that was enhanced by agonists, and diminished by antagonists, of TRPV1. Cochlear TRPV1 was immunolocalized near the apical membranes of sensory hair cells, adjacent supporting cells, and marginal cells in the stria vascularis. Exposure to immunostimulatory lipopolysaccharides, to simulate of bacterial infections, increased cochlear expression of TRPV1 and hair cell uptake of gentamicin. Lipopolysaccharide exposure exacerbated aminoglycoside-induced auditory threshold shifts and loss of cochlear hair cells in wild-type, but not in heterozygous *Trpv1*$^{+/-}$ or *Trpv1* knockout, mice. Thus, TRPV1 facilitates cochlear uptake of aminoglycosides, and bacteriogenic stimulation upregulates TRPV1 expression to exacerbate cochleotoxicity. Furthermore, loss-of-function polymorphisms in *Trpv1* can protect against immunogenic exacerbation of aminoglycoside-induced cochleotoxicity.

INTRODUCTION

Aminoglycoside antibiotics, like gentamicin, are clinically essential pharmacotherapeutics to treat severe bacterial infections due to their efficacy and low cost (*1*). Inner ear uptake of aminoglycosides can lead to sensory hair cell death and lifelong hearing loss (*1*–*3*), resulting in huge socioeconomic costs in acquiring listening and spoken language skills, or achieving academic milestones that influence quality-of-life measures for affected individuals (*4*). Notably, bacteriogenic induction of inflammation exacerbated aminoglycoside-induced hearing loss (cochleotoxicity) in mice (*5*) and potentially in humans (*6*). Thus, the very patients with severe systemic infections (and thus inflammation) treated with lifesaving aminoglycosides have a higher risk of drug-induced cochleotoxicity. The mechanisms by which inflammation exacerbates aminoglycoside-induced cochleotoxicity remain undetermined.

The hydrophilic aminoglycosides predominantly enter inner ear sensory hair cells by permeating the mechanoelectrical transduction channel, TMC1 (*7*, *8*), as well as via endocytosis (*9*). The transient receptor potential vanilloid (TRPV) channel family contains six nonselective cation channels, of which one—TRPV1—can be activated by capsaicin, the pungent component of chili peppers (*10*). Agonists and antagonists of TRPV1 can mediate cellular uptake of fluorescent gentamicin (*11*). In the rodent cochlea, TRPV1 is expressed in the stria vascularis, as well as in inner and outer hair cells (IHC and OHC, respectively) (*12*, *13*), key locations in the trafficking of aminoglycosides from the bloodstream into sensory hair cells (*14*). Inflammatory signaling pathways up-regulate cochlear expression of TRPV1 (*15*). Therefore, we tested the hypotheses that induced TRPV1 expression (i) facilitates cellular uptake of aminoglycosides and cytotoxicity in vitro, (ii) enhances hair cell uptake of aminoglycosides during systemic inflammation in vivo, and (iii) exacerbates aminoglycoside-induced cochleotoxicity. Our data here support these hypotheses.

RESULTS

TRPV1 expression analysis and TRPV1 cell line generation

In immunoblots of lysed kidney cell lines using TRPV1 antisera, mouse kidney proximal tubule [KPT, clone 2 and 11 (KPT2 and KPT11)] cells exhibited weak band densities at ~95 kDa, the expected molecular mass of TRPV1 (*10*). Cell lysates from murine kidney distal tubule [KDT, clone 3 (KDT3)] and mouse distal convoluted tubule (MDCT) cells exhibited stronger band densities at ~95 kDa (Fig. 1A and fig. S1A). Similarly, TRPV1 immunofluorescence was present in KPT11 and MDCT cells, with little fluorescence in KPT2 and KDT3 cells (Fig. 1B). Stable cell lines expressing TRPV1 were generated using KPT2 cells. Four KPT2-derived cell lines expressing TRPV1 (KPT2-*Trpv1*) and three empty retroviral vector control cell lines (KPT2-pBabe) all retained the parental KPT2 epithelioid morphology (fig. S1B). In immunoblots, control KPT2-pBabe cells had very weak, or nonspecific, band density compared to two TRPV1-expressing KPT2-*Trpv1* clones with strong band densities at ~95 kDa (fig. S1C). Immunofluorescence revealed robust TRPV1 immunofluorescence in KPT2-*Trpv1*, but not in KPT2-pBabe, cells (Fig. 1C).

Activation of TRPV1 enhances cellular uptake of gentamicin

To assess the permeability of heterologously expressed TRPV1 to gentamicin, we incubated KPT2-*Trpv1* or KPT2-pBabe cells with fluorescent gentamicin (5 μg/ml) [gentamicin conjugated to Texas Red (GTTR)] for 60 s before fixation and confocal microscopy. Greater GTTR fluorescence was present in KPT2-*Trpv1* cells compared to control KPT2-pBabe cells lacking TRPV1 immunofluorescence ($P < 0.05$; Fig. 2, A and B). The TRPV1 agonist resiniferatoxin

[1]Oregon Hearing Research Center, Oregon Health & Science University, 3181 SW Sam Jackson Park Road, Portland, OR 97239, USA. [2]National Center for Rehabilitative Auditory Research, VA Portland Health Care System, Portland, OR 97239, USA.
*These authors contributed equally to this work as co-first authors.
†Present address: Research Service, VA Loma Linda Healthcare System, Loma Linda, CA 92357, USA.
‡Corresponding author. Email: petersteyger@creighton.edu
§Present address: Translational Hearing Center, Department of Biomedical Sciences, Creighton University, Omaha, NE 68178, USA.

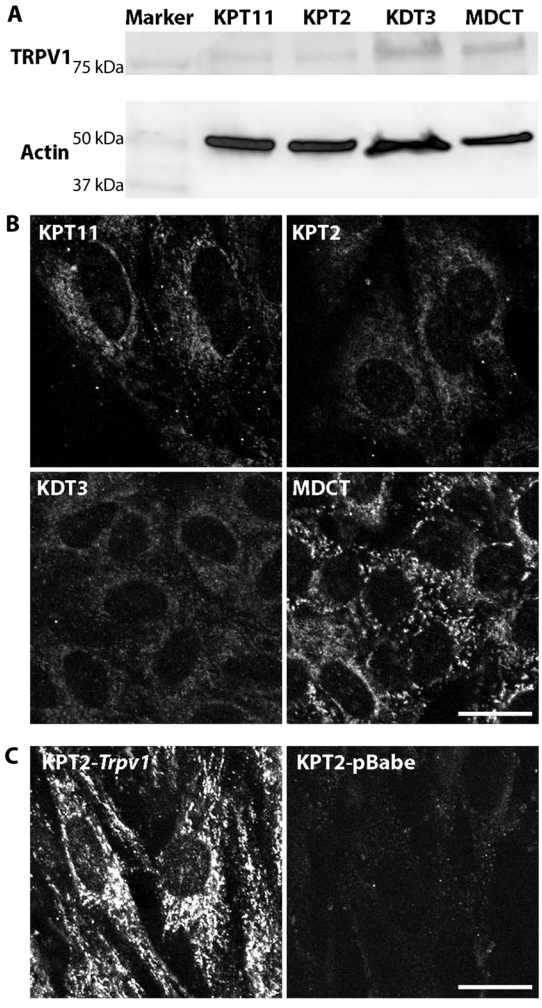

Fig. 1. TRPV1 immunoexpression in cell lines. (**A**) Immunoblot of lysates from kidney cell lines using TRPV1 antisera (cat# ACC-030; Alomone Labs). At ~95 kDa, the expected molecular mass of TRPV1, KPT2, and KPT11 cells exhibited weak band densities, while KDT3 and MDCT cells had strong band densities. At ~42 kDa, immunolabeling for actin served as a loading control. (**B**) TRPV1 immunofluorescence was detected in KPT11 and MDCT cells, with negligible fluorescence in KPT2 and KDT3 cells. (**C**) Robust TRPV1 immunofluorescence is present in KPT2-*Trpv1*, but not in control KPT2-pBabe, cells. Scale bars, 20 μm.

(RTX) significantly enhanced GTTR fluorescence in KPT2-*Trpv1* cells compared to KPT2-*Trpv1* cells without RTX treatment ($P < 0.05$; Fig. 2, A and B). RTX also significantly enhanced GTTR fluorescence in KPT2-*Trpv1* cells compared to KPT2-pBabe cells with RTX treatment ($P < 0.05$; Fig. 2, A and B). GTTR fluorescence in RTX-treated KPT2-pBabe cells was similar to KPT2-pBabe cells without RTX treatment ($P > 0.05$; Fig. 2, A and B). Iodo-RTX (I-RTX; the inert form of RTX and an antagonist of TRPV1) significantly reduced GTTR fluorescence in KPT2-*Trpv1* cells compared to KPT2-*Trpv1* cells without I-RTX ($P < 0.05$; Fig. 2, A and B). GTTR fluorescence in I-RTX–treated KPT2-*Trpv1* cells was similar to KPT2-pBabe cells with or without I-RTX treatment ($P > 0.05$; Fig. 2, A and B). To validate imaging data, we used enzyme-linked immunosorbent assays (ELISAs). Significantly increased levels of GTTR (Fig. 2C) and native gentamicin (Fig. 2D) were observed in (i) KPT2-*Trpv1* cells compared to KPT2-pBabe cells, (ii) RTX-treated KPT2-*Trpv1* cells compared to RTX-treated KPT2-pBabe cells or untreated KPT2-*Trpv1* cells, and (iii) KPT2-*Trpv1* cells compared to I-RTX–treated KPT2-*Trpv1* or KPT2-pBabe cells ($P < 0.05$). These data support the hypothesis that TRPV1 facilitates gentamicin entry into cells, as also reported for TRPV4 channels (*16*).

TRPV1-mediated uptake of gentamicin is attenuated by extracellular [Ca^{2+}]

Cation flux through TRPV1 (and other TRPV) channels is modulated by extracellular concentrations of Ca^{2+} (*10*, *16*). KPT2-*Trpv1* cells treated with GTTR in culture media with 2 mM extracellular [Ca^{2+}] had significantly reduced GTTR fluorescence compared to cells in culture media without extracellular [Ca^{2+}] ($P < 0.05$; Fig. 3, A and B). Extracellular [Ca^{2+}] (2 mM) did not modulate TR fluorescence in KPT2-pBabe cells (Fig. 3, B and D). TRPV1 agonists (capsaicin and RTX) significantly increased GTTR fluorescence in KPT2-*Trpv1* cells but not in KPT2-pBabe cells ($P < 0.05$; Fig. 3, A and B and fig. S2). Agonist-enhanced GTTR uptake in KPT2-*Trpv1* cells could be significantly attenuated by 2 mM extracellular [Ca^{2+}] ($P < 0.05$; Fig. 3, A and B, and fig. S2). ELISA data for cellular levels of GTTR and native gentamicin validated imaging data, including significant attenuation of RTX-enhanced cellular uptake of aminoglycosides in KPT2-*Trpv1* cells by 2 mM extracellular [Ca^{2+}] ($P < 0.05$; Fig. 3, C and D and fig. S2). These data support the hypothesis that TRPV1 facilitates gentamicin entry into cells and that the TRPV1-mediated cellular uptake of gentamicin can be modulated by extracellular [Ca^{2+}], suggestive of permeation through the TRPV1 channel pore, as for TRPV4 (*16*).

Activation of heterologous TRPV1 exacerbates gentamicin-induced cytotoxicity

Caterina *et al.* (*10*) reported that capsaicin potentiated cytotoxicity in cells heterologously expressing TRPV1. These cells were incubated in culture media supplemented with the aminoglycoside antibiotic streptomycin for prophylaxis against bacterial contamination. To test whether aminoglycosides are more cytotoxic when TRPV1 is activated, we used a 3-(4,5-dimethylthiazol-2-yl)-2,5-diphenyltetrazolium bromide (MTT) colorimetric assay for cell viability (*17*). The viability of parental KPT2, KPT2-pBabe, or KPT2-*Trpv1* cells was not significantly altered when exposed to capsaicin or capsazepine alone (3 or 15 μM; fig. S3A). Incubation with 10 mM gentamicin for 3 hours did not significantly reduce the viability of KPT2, KPT2-pBabe, and KPT2-*Trpv1* cells (Fig. 4A). KPT2-*Trpv1* (but not KPT2 or KPT2-pBabe) cells were significantly more susceptible to gentamicin-induced cytotoxicity in the presence of TRPV1 agonist capsaicin ($P < 0.05$) but not when gentamicin-treated cells were coincubated with capsazepine, a TRPV1 antagonist (Fig. 4A and fig. S3B).

MDCT cells with endogenous expression of TRPV1 (Fig. 1) were susceptible to incubation with 10 mM gentamicin for 3 hours, and this cytotoxicity could be significantly attenuated when coincubated with capsazepine ($P < 0.05$; fig. S3B). Capsaicin significantly exacerbated gentamicin-induced cytotoxicity in MDCT cells ($P < 0.05$; fig. S3B). Thus, expression and activation of TRPV1 exacerbate gentamicin-induced cytotoxicity, further implicating the involvement of TRPV1 in cellular uptake of gentamicin and subsequent drug-induced cytotoxicity. Agonists and antagonists of TRPV1 do not affect the bactericidal efficacy of aminoglycosides (fig. S4).

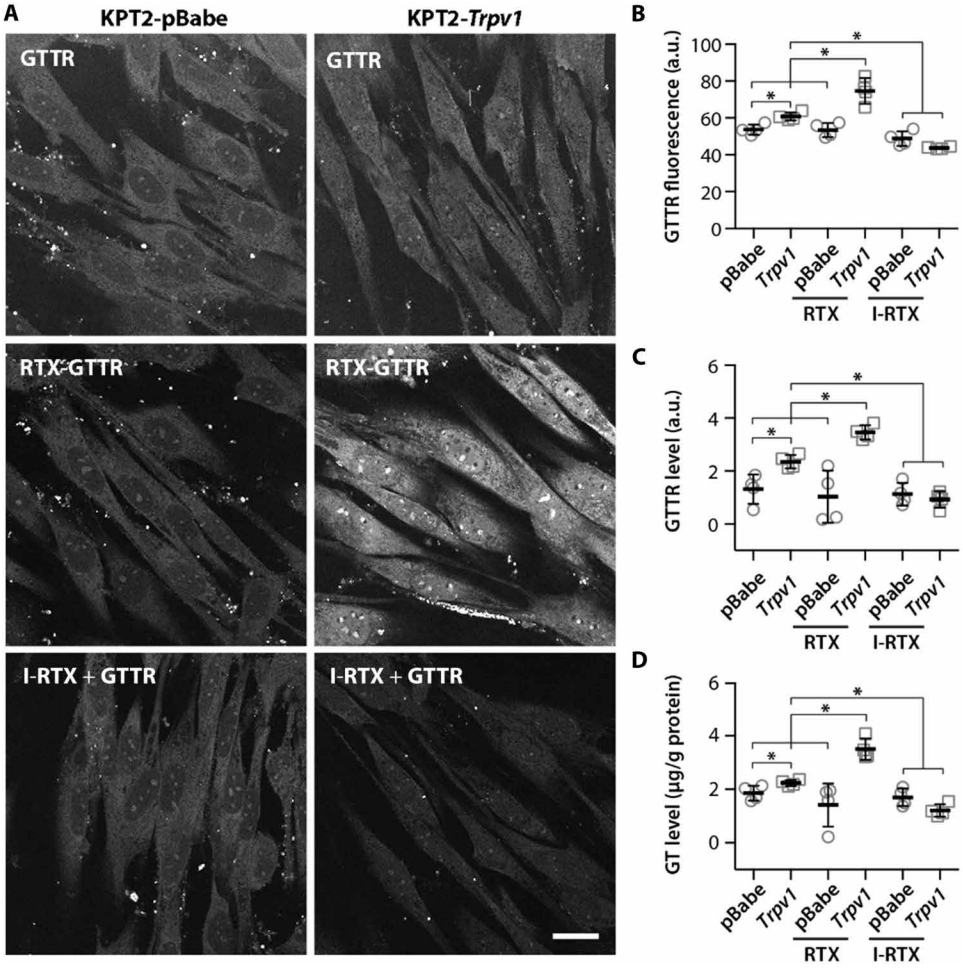

Fig. 2. Activation of heterologously expressed TRPV1 enhanced cellular uptake of gentamicin. (**A**) Following 1-min incubation with GTTR, KPT2-*Trpv1* cells display more GTTR fluorescence compared to KPT2-pBabe cells. KPT2-*Trpv1* cells treated with RTX (5 nM) exhibit increased GTTR fluorescence compared to RTX-treated KPT2-pBabe cells or KPT2-*Trpv1* cells treated with GTTR only. Weak GTTR fluorescence in I-RTX–treated KPT2-*Trpv1* cells was similar in intensity to KPT2-pBabe cells treated with GTTR only or with a TRPV1 antagonist (I-RTX, 100 nM) and was visibly less intense than in KPT2-*Trpv1* cells treated with GTTR only. Scale bar, 20 µm. (**B**) Significantly increased pixel intensities for GTTR fluorescence in (i) KPT2-*Trpv1* cells compared to KPT2-pBabe cells; (ii) RTX-treated KPT2-*Trpv1* cells compared to RTX-treated KPT2-pBabe cells, non-RTX–treated KPT2-*Trpv1* cells, or non-RTX–treated KPT2-pBabe cells; and (iii) KPT2-*Trpv1* cells compared to I-RTX–treated KPT2-*Trpv1* cells and I-RTX–treated KPT2-pBabe cells (*$P < 0.05$; $n = 4$ per group). ELISAs revealed significantly increased levels of GTTR (**C**) and native gentamicin (**D**) in (i) KPT2-*Trpv1* cells compared to KPT2-pBabe cells; (ii) RTX-treated KPT2-*Trpv1* cells compared to RTX-treated KPT2-pBabe cells, and untreated KPT2-*Trpv1* or KPT2-pBabe cells; and (iii) KPT2-*Trpv1* cells compared to I-RTX–treated KPT2-*Trpv1* or KPT2-pBabe cells (*$P < 0.05$; $n = 4$ per group). Error bars, SD. a.u., arbitrary units.

Knockdown of TRPV1 mitigates gentamicin-induced cytotoxicity

Since activated TRPV1 exacerbates gentamicin-induced cytotoxicity, we wondered whether knockdown of endogenous TRPV1 in MDCT cells (Fig. 1, A and B) mitigated gentamicin-induced cytotoxicity. In MDCT cells transfected with control small interfering RNA (siRNA), TRPV1 immunofluorescence remained robust, while transfection with siRNA for TRPV1 robustly knocked down visible TRPV1 immunofluorescence (Fig. 4B). Expression of RNA for TRPV1 in MDCT cells was significantly diminished by siRNA for TRPV1 ($P < 0.05$; Fig. 4C). Transfection with siRNA for TRPV1 did not affect cell viability compared to control siRNA-transfected cells (Fig. 4D). siRNA knockdown of TRPV1 significantly ameliorated the degree of gentamicin-induced cytotoxicity ($P < 0.05$; Fig. 4D). Thus, endogenous TRPV1 expression levels modulate gentamicin-induced cytotoxicity. In toto, our in vitro data implicate a pivotal role for TRPV1 in cellular uptake of gentamicin and subsequent cytotoxicity.

TRPV1 expression in the kidney and cochlea

In vibratome sections of wild-type kidneys, TRPV1 immunofluorescence is prominently localized in the apical brush border of proximal tubule cells, as well as the soma of proximal and distal tubule cells (Fig. 5A), and less intensely in glomerular cells (fig. S5). Negligible immunofluorescence is present in kidney cells following incubation with antigen-adsorbed TRPV1 antibodies (Fig. 5A).

In the stria vascularis, TRPV1 is strongly immunolocalized near the lumenal surface of marginal cells, with weak labeling in intermediate cells (Fig. 5, B and C). Stronger, more punctate TRPV1 immunolabeling is present in basal cells and fibrocytes (Fig. 5, B and C). Negligible fluorescence was present in strial cells or fibrocytes following incubation with antigen-adsorbed TRPV1 antibodies (Fig. 5B). In the organ of

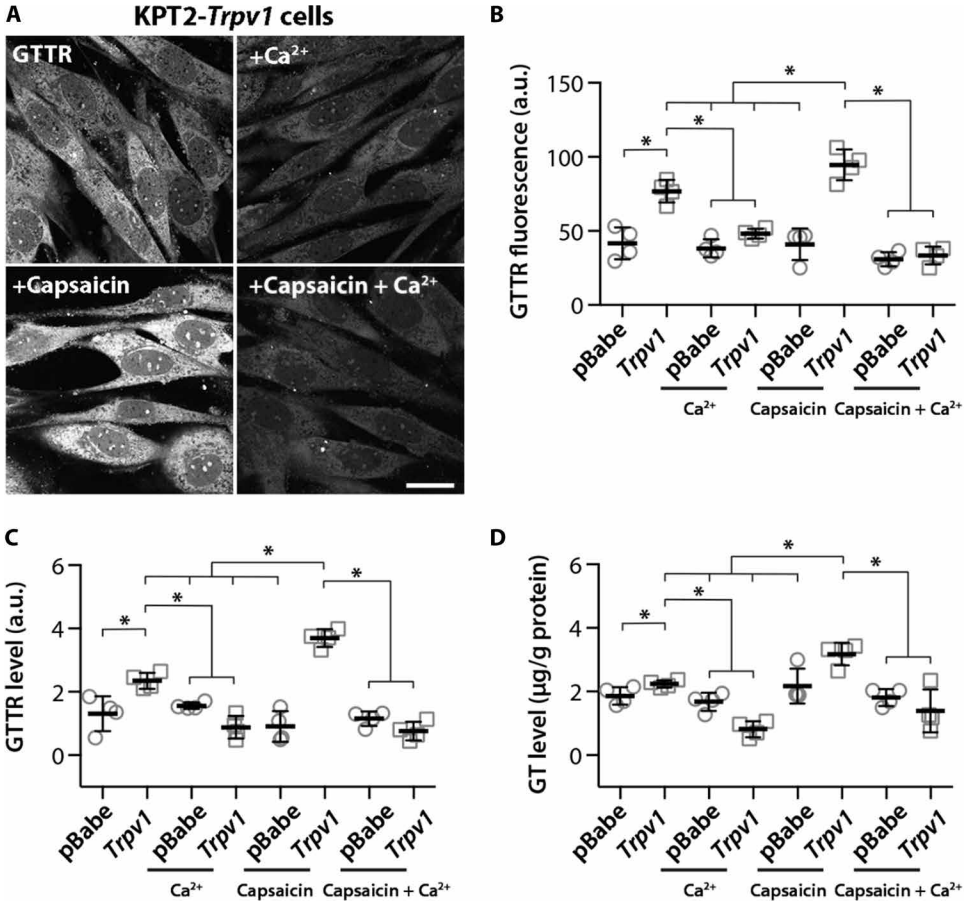

Fig. 3. Heterologous TRPV1-mediated uptake of gentamicin is attenuated by extracellular [Ca^{2+}]. (**A**) KPT2-*Trpv1* cells treated with GTTR (5 μg/ml) show reduced fluorescence when coincubated with 2 mM extracellular [Ca^{2+}]. The TRPV1 agonist capsaicin (3 μM) visibly increased GTTR fluorescence over untreated KPT2-*Trpv1* cells. Capsaicin-enhanced GTTR uptake is visibly attenuated by 2 mM extracellular [Ca^{2+}]. Scale bar, 20 μm. (**B**) GTTR fluorescence in KPT2-pBabe cells was significantly less than that in KPT2-*Trpv1* cells. Extracellular [Ca^{2+}] (2 mM) diminished GTTR fluorescence in KPT2-*Trpv1* cells. Capsaicin significantly increased GTTR fluorescence in KPT2-*Trpv1* cells but not in KPT2-pBabe cells. Capsaicin-enhanced GTTR uptake in KPT2-*Trpv1* cells is significantly attenuated by 2 mM extracellular [Ca^{2+}], without modulating GTTR levels in KPT2-pBabe cells ($P > 0.05$; $n = 4$ per group). ELISA data for cellular levels of GTTR (**C**) and native gentamicin (**D**) support imaging data described in (A) and (B) (*$P < 0.05$; $n = 4$ per group). Error bars, SD.

Corti, punctate TRPV1 immunofluorescence is present at the level of the cuticular plate, reminiscent of the cytoplasmic channels through the cuticular plate of OHCs (*18*, *19*). Similar labeling patterns also occur around the periphery of the IHC apices and on the modiolar side of IHCs, close to the cuticular plate (Fig. 5D), akin to the previously described distribution of microtubules adjacent to the cuticular plate (*18*, *19*). The cuticular plates of IHCs and OHCs are less intensely labeled for TRPV1 (Fig. 5D), with less intense labeling in the hair cell bodies (not shown). In supporting cells, more intense TRPV1 immunofluorescence is localized in the inner pillar cell phalanges, outer pillar cell phalanges, and Deiters' cell phalanges (Fig. 5D), as for guinea pigs (*12*).

LPS enhances TRPV1 expression and hair cell uptake of GTTR in cochlear coil explants

In preclinical models, cisplatin up-regulated cochlear expression of TRPV1 (*13*). TRPV1 agonists exacerbated cisplatin-induced cochleotoxicity, and conversely, knockdown of TRPV1 expression attenuated cisplatin-induced cytotoxicity (*20*). Since exposure to bacterial lipopolysaccharides (LPS) increased cochlear uptake of aminoglycosides (*5*), we examined whether LPS exposure increased cochlear expression of TRPV1 and uptake of GTTR by hair cells. To best assess whether hair cell uptake of GTTR can be mediated by TRPV1, we explanted murine neonatal cochlear coils (*21*) from *Pcdh15* knockout (KO) pups that lack protocadherin-15 (*22*). Protocadherin-15 is an essential component of stereociliary tiplinks that mechanically gate the aminoglycoside-permeant TMC1 channels expressed by inner ear sensory hair cells (*7*, *22*, *23*).

In cochlear coil explants from heterozygous *Pcdh15*$^{+/-}$ and *Pcdh15* KO pups, strong TRPV1 immunofluorescence is present at the phalangeal apices of Deiters' cells, as well as inner and outer pillar cells (Fig. 6, A and B), similar to that described for adult wild-type mice (Fig. 5). IHC apices displayed less intense TRPV1 immunofluorescence than supporting cell apices, with weaker expression in OHC apices (Fig. 6, A and B). Twenty-four hours after a 1-hour exposure to LPS (1 μg/ml), significantly increased TRPV1 immunofluorescence was present for these cell types in both *Pcdh15*$^{+/-}$ and *Pcdh15* KO cochlear coil explants ($P < 0.05$; Fig. 6B).

In cochlear coil explants incubated with GTTR for 30 min before fixation, GTTR fluorescence was visibly more intense in *Pcdh15*$^{+/-}$

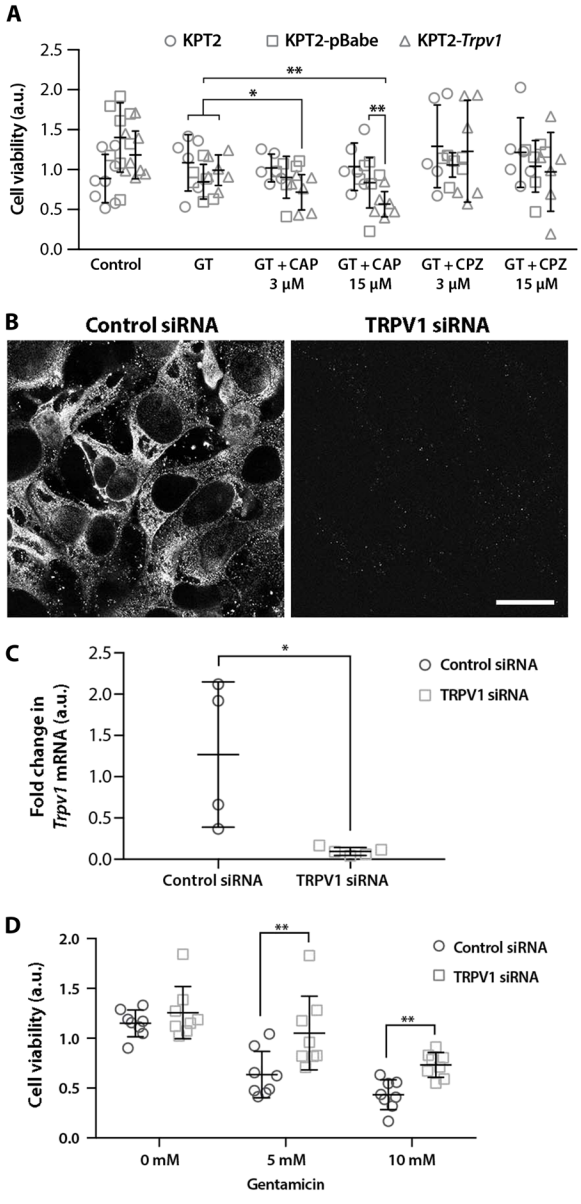

Fig. 4. Activation of heterologous TRPV1 exacerbated gentamicin-induced cytotoxicity. (**A**) KPT2-*Trpv1* cells are more susceptible to 10 mM gentamicin (GT) treatment for 3 hours in the presence of TRPV1 agonist capsaicin (CAP; **P* < 0.05; ***P* < 0.01) but not when coincubated with a TRPV1 antagonist, capsazepine (CPZ). The viability of parental KPT2 or KPT2-pBabe cells (without heterologous TRPV1 expression) was not significantly altered by GT alone or by GT in the presence of capsaicin or capsazepine. (**B**) Strong TRPV1 immunofluorescence in MDCT cells (transfected with control siRNA) was greatly diminished in MDCT cells transfected with siRNA for TRPV1. Scale bar, 20 μm. (**C**) Expression of *Trpv1* RNA in MDCT cells is significantly diminished by siRNA for *Trpv1* (**P* < 0.05; *n* ≥ 4). (**D**) MDCT cells transfected with siRNA for TRPV1 and then treated with GT were significantly more viable than MDCT cells transfected with control siRNA (***P* < 0.01; *n* = 8). Error bars, SD.

OHCs and IHCs than in hair cells from *Pcdh15* KO mice ($P < 0.0001$; Fig. 6C), consistent with a loss of TMC1 conductance in *Pcdh15* KO explants (*22*) and, consequently, reduced GTTR permeation of TMC1 channels. Exposure to LPS significantly increased GTTR fluorescence in OHCs and IHCs in *Pcdh15*$^{+/-}$ and *Pcdh15* KO explants compared to explants without LPS exposure ($P < 0.0001$; Fig. 6, C and D). TRPV1 immunofluorescence was also significantly up-regulated in pillar cells between the OHCs and IHCs in *Pcdh15*$^{+/-}$ and *Pcdh15* KO explants ($P < 0.05$; Fig. 6, A and B). Similarly, enhanced GTTR fluorescence was visible in pillar cells following LPS exposure compared to control explants from *Pcdh15*$^{+/-}$ and *Pcdh15* KO mice (Fig. 6C), suggestive of *Trpv1*-facilitated GTTR uptake; however, this did not reach statistical significance. Thus, LPS up-regulated the expression of TRPV1 at the reticular lamina of organ of Corti explants and increased OHC uptake of GTTR. Furthermore, the LPS-enhanced uptake of GTTR was substantially greater in *Pcdh15*$^{+/-}$ OHCs than in OHCs from *Pcdh15* KO cochlear explants, suggesting that LPS exposure, and/or greater TRPV1 expression, modulated TMC1 channel conductance and thereby GTTR entry kinetics into OHCs.

LPS-enhanced cochlear TRPV1 expression and GTTR uptake in vivo are dependent on TLR4

In *Pcdh15* KO mice, OHCs begin to degenerate a few weeks after birth (*24*), precluding in vivo experiments with *Pcdh15* KO mice in vivo. Since LPS sensitizes, and up-regulates expression of, TRPV1 via Toll-like receptor 4 (TLR4) signaling (*15*, *25*), we assessed whether LPS up-regulated cochlear (and renal) expression of TRPV1 and enhanced OHC uptake of GTTR in wild-type, *TLR4* KO, or *Trpv1* KO mice in vivo. Twenty-four hours after intravenous (i.v.) injection, LPS (1 mg/kg) significantly enhanced cochlear immunoexpression of TRPV1 in the marginal cells and reticular lamina of wild-type, but not *Tlr4* KO, cochleae ($P < 0.05$; Fig. 7, A to D) or spiral ganglion cells (data not shown). LPS exposure substantially enhanced TRPV1 immunolabeling in renal tubular cells (fig. S5). In addition, LPS increased *Trpv1* mRNA expression in wild-type, but not in *Tlr4* KO, cochleae ($P < 0.05$; Fig. 7E). Similarly, LPS increased *Trpv1* mRNA expression in wild-type, but not in *Trpv1* KO, cochleae ($P < 0.01$; Fig. 7F). LPS also increased GTTR fluorescence in wild-type OHCs but not OHCs in *Trpv1* KO mice ($P < 0.0001$; Fig. 7, G and H). Similarly, LPS treatment enhanced uptake of GTTR by marginal cells of the stria vascularis of wild-type mice (Fig. 7B) but not *Trpv1* KO mice (fig. S6).

LPS exacerbates kanamycin-induced hearing loss in wild-type, but not in Trpv1$^{+/-}$ or Trpv1 KO, mice

Since systemic LPS exposure increased cochlear expression of TRPV1, OHC, and marginal cell uptake of aminoglycosides (Fig. 7), as well as cochleotoxicity (*5*), we hypothesized that *Trpv1* KO mice would have reduced auditory brainstem response (ABR) threshold shifts following aminoglycoside treatment compared to wild-type mice. As chronic dosing with gentamicin is systemically lethal to mice, we used a validated ototoxicity protocol using a related aminoglycoside, kanamycin (*3*, *5*). For each murine strain (wild-type C57BL/6; heterozygous *Trpv1*$^{+/-}$ or *Trpv1* KO), one group received LPS (1 mg/kg, i.v.) the day before kanamycin treatment and on the 5th and 10th day during a 15-day course of kanamycin treatment (850 mg/kg, twice daily). ABR thresholds were obtained from age-matched mice 21 days after injections, and shifts from baseline were determined (Fig. 8). The 3-week post-treatment time point is an established benchmark for determining permanent threshold shifts (PTS) in preclinical ototoxicity studies (*3*, *5*).

Three weeks after Dulbecco's phosphate-buffered saline (DPBS) treatment, wild-type and *Trpv1*$^{+/-}$ mice had significant threshold shifts ($P < 0.01$) at all frequencies (except 16 kHz; see tables S1 and

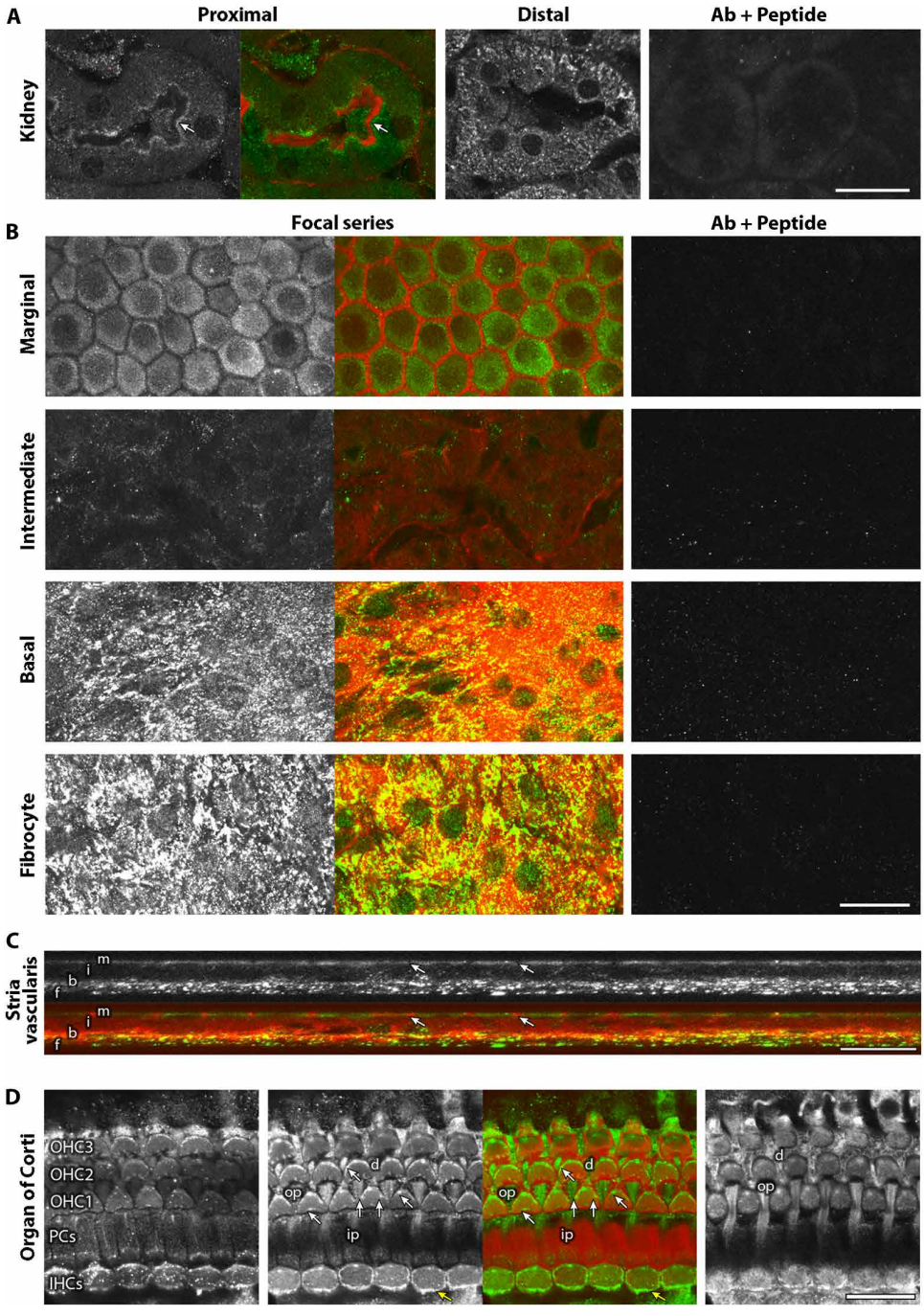

Fig. 5. TRPV1 expression in kidney and inner ear. (**A**) In wild-type mice, TRPV1 immunofluorescence (green in color images) is present (arrows) near the apical brush border (red in color images) of proximal tubule cells, as well as in the soma of proximal, and as puncta in distal, tubule cells. Negligible immunofluorescence when the TRPV1 antibody was adsorbed with the antigenic peptide. Ab, antibody. (**B**) In whole mounts of the cochlear lateral wall, specific TRPV1 immunofluorescence near the lumenal surface of marginal cells (white or green) at the level of the actiniferous tight junctions (red) between adjacent marginal cells. Weak TRPV1 immunolabeling in intermediate cells, with stronger, more punctate, labeling in basal cells and fibrocytes. Negligible fluorescence detected in strial cells or fibrocytes when the TRPV1 antibody is adsorbed with the antigenic peptide. (**C**) In *z*-sections of the stria vascularis, TRPV1 immunofluorescence (green in the lower panel) is localized near the lumenal surface of the marginal cells (m), between the actiniferous tight junctions (red in the lower panel, arrows), and in basal cells (b) and fibrocytes (f) below the weakly labeled soma of intermediate (i) cells. (**D**) In the organ of Corti, punctate TRPV1 immunofluorescence (green, vertical arrows) is present in cytoplasmic channels in the cuticular plate, as well as a stripe near the lateral side (diagonal arrows), of OHCs. TRPV1 immunofluorescence is also localized in the inner pillar cell phalanges (ip) between IHCs and OHCs, outer pillar cell phalanges (op) between OHCs of the first row, and Deiters' cells phalanges (d) between OHCs in row 2 and row 3 of OHCs. TRPV1 immunolabeling also lines the periphery of IHCs, especially on the modiolar side of IHC (yellow arrows). Scale bars, 20 μm.

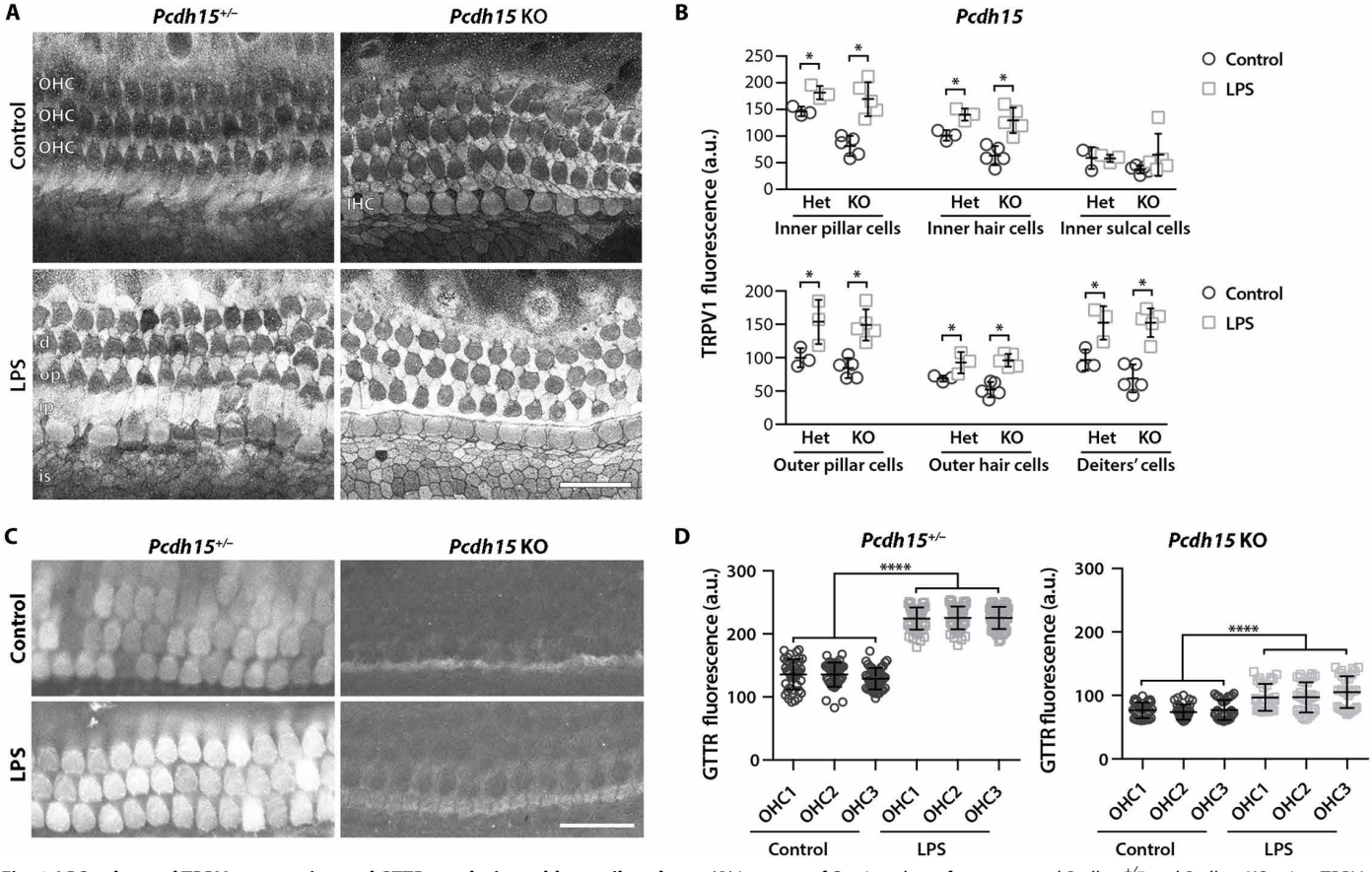

Fig. 6. LPS enhanced TRPV1 expression and GTTR uptake in cochlear coil explants. (**A**) In organ of Corti explants from neonatal *Pcdh15*$^{+/-}$ and *Pcdh15* KO mice, TRPV1 immunofluorescence was visibly more intense in the phalangeal apices of inner and outer pillar cells (ip and op, respectively), as well as Deiters' cells (d), compared to IHC, and especially OHC, apices and inner sulcal cells (is). Twenty-four hours after a 1-hour exposure to LPS (1 μg/ml), enhanced TRPV1 immunofluorescence is observed throughout organ of Corti explants from *Pcdh15*$^{+/-}$ and *Pcdh15* KO mice compared to untreated explants. (**B**) LPS significantly increased the pixel intensity of TRPV1 immunofluorescence in inner pillar cells, IHCs, outer pillar cells, OHCs, and Deiters' cells, but not in inner sulcus cells, in organ of Corti explants from *Pcdh15*$^{+/-}$ (Het) and *Pcdh15* KO (KO) mice over that in non–LPS-treated cochlear coils (*$P < 0.05$; $n \geq 3$). (**C**) In untreated explants incubated with GTTR for 5 min, GTTR fluorescence was visibly more intense in *Pcdh15*$^{+/-}$ OHCs and IHCs than in control hair cells from *Pcdh15* KO mice. GTTR fluorescence is also visible in pillar cells between the OHCs and IHCs, especially in *Pcdh15* KO explants. Twenty-four hours after exposure to LPS, enhanced GTTR fluorescence is observed in *Pcdh15*$^{+/-}$ OHCs, IHCs, and pillar cell apices compared to control *Pcdh15*$^{+/-}$ explants. Enhanced GTTR fluorescence is also observed in OHCs, IHCs, and pillar cell apices of *Pcdh15* KO explants exposed to LPS compared to control *Pcdh15* KO explants. (**D**) LPS exposure significantly increased the intensity of GTTR fluorescence in OHCs of both *Pcdh15*$^{+/-}$ and *Pcdh15* KO cochlear explants (****$P < 0.0001$; $n \geq 3$). Scale bars, 20 μm. Error bars, SD.

S2 for all *P* values), likely due to early onset of age-related hearing loss (*26*). *Trpv1* KO mice had significant threshold shifts only at higher frequencies, i.e., at 24, 32, and 48 kHz, compared to pretreatment baselines ($P < 0.01$; table S3). These PTS generally did not differ significantly between strains, although *Trpv1*$^{+/-}$ mice differed significantly from other strains at 12 and 32 kHz ($P < 0.001$; Fig. 8A and table S4). After LPS treatment, *Trpv1* KO mice had significantly greater PTS at 48 kHz than other strains ($P < 0.001$; Fig. 8A and table S5). Three weeks after kanamycin treatment, wild-type mice generally had significantly greater threshold shifts compared to *Trpv1*$^{+/-}$ mice, as did *Trpv1* KO mice over *Trpv1*$^{+/-}$ mice at 12 and 16 kHz ($P < 0.05$; Fig. 8A and table S6). Following LPS + kanamycin treatment, wild-type mice had significantly greater threshold shifts at all frequencies compared to *Trpv1*$^{+/-}$ or *Trpv1* KO mice, except at 32 and 48 kHz ($P < 0.05$; Fig. 8A and table S7; fig. S7 and tables S8 to S10 compare treatment groups for each mouse strain). Thus, wild-type mice are more susceptible to kanamycin-induced ototoxicity than *Trpv1*$^{+/-}$ or *Trpv1* KO mice, especially in the presence of LPS-induced inflammation. Notably, in acute studies, wild-type mice did not have greater cochlear uptake of kanamycin compared to *Trpv1*$^{+/-}$ or *Trpv1* KO mice (fig. S10), suggesting that the kinetics of aminoglycoside entry into cochlear tissues is not dependent on expression of functional TRPV1. Furthermore, the LPS-enhanced uptake of gentamicin seen in wild-type mice, as previously described (*5*), is not replicated in *Trpv1*$^{+/-}$ or *Trpv1* KO mice (fig. S8), suggesting that LPS-enhanced expression or activity of TRPV1 contributes to the potentiation of aminoglycoside-induced cochleotoxicity in wild-type mice.

LPS exacerbates kanamycin-induced OHC death in wild-type, but not in Trpv1$^{+/-}$ or Trpv1 KO, mice

To further verify whether TRPV1 contributes to LPS-exacerbated kanamycin-induced hair cell death, we determined OHC survival rates in wild-type, *Trpv1*$^{+/-}$, and *Trpv1* KO cochleae 21 days after treatment

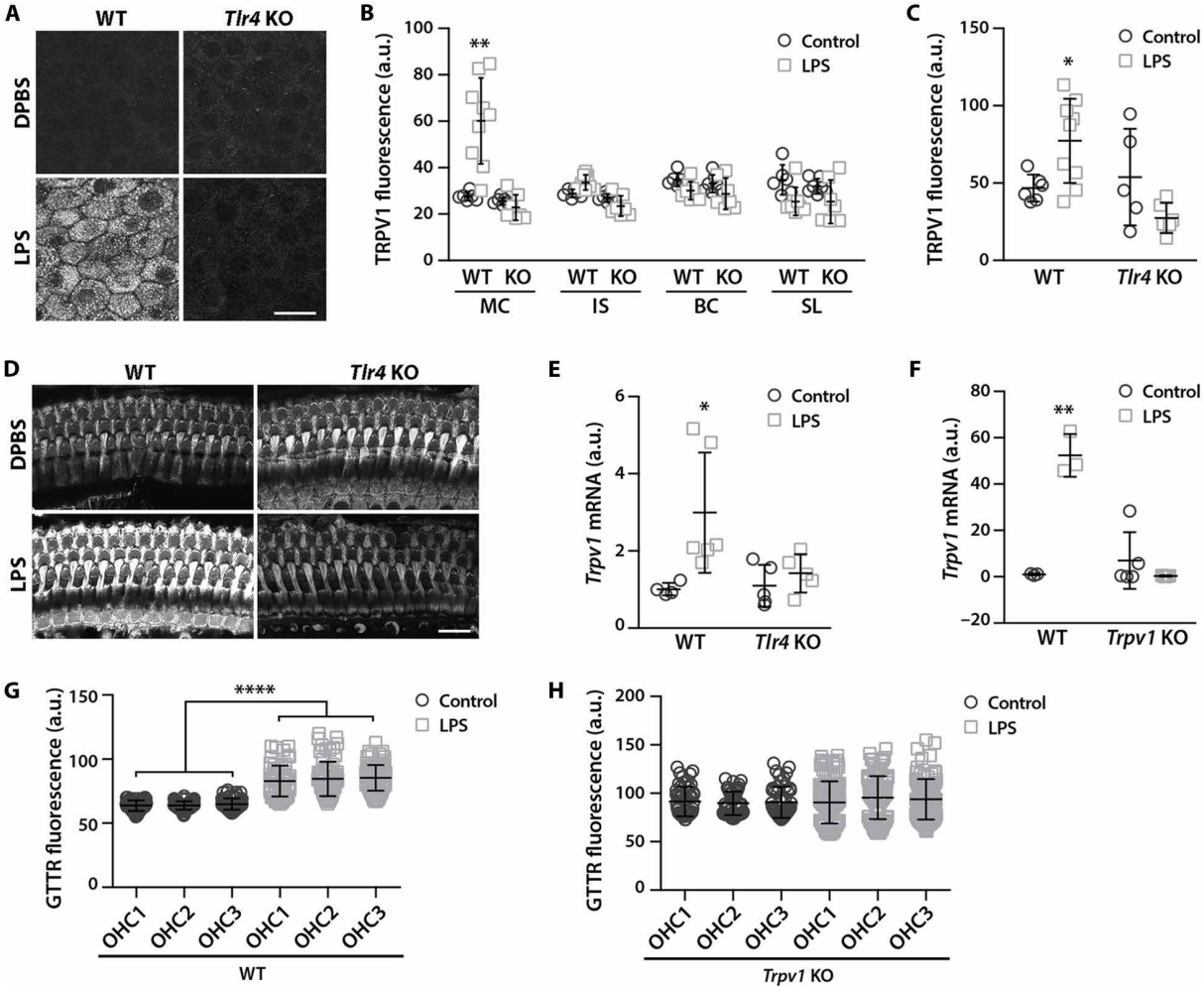

Fig. 7. LPS enhances cochlear TRPV1 expression and GTTR uptake in vivo. (**A**) LPS enhanced TRPV1 expression in wild-type (WT) marginal cells compared to DPBS-treated wild-type mice. LPS did not enhance TRPV1 expression in marginal cells of *Tlr4* KO mice. (**B**) LPS significantly enhanced TRPV1 immunofluorescence in marginal cells (MC) of wild-type, but not *Tlr4* KO, mice (**$P < 0.01$; $n \geq 6$). TRPV1 immunofluorescence in intra-strial (IS) and basal cells (BC), as well as spiral ligament fibrocytes (SL), was not significantly altered. (**C**) LPS significantly enhanced TRPV1 immunofluorescence in OHCs of wild-type, but not *Tlr4* KO, mice (*$P < 0.05$; $n \geq 5$). (**D**) LPS enhanced TRPV1 expression in the reticular lamina of wild-type mice compared to DPBS-treated wild-type mice. LPS did not enhance TRPV1 expression in the organ of Corti of *Tlr4* KO mice. (**E**) Significantly increased *Trpv1* mRNA expression in the cochleae of wild-type, but not in *Tlr4* KO, cochleae following LPS exposure (*$P < 0.05$; $n \geq 5$). (**F**) Significantly increased *Trpv1* mRNA expression in the cochleae of wild-type, but not *Trpv1* KO, cochleae following LPS exposure (**$P < 0.01$; $n \geq 3$). (**G**) Intravenous LPS 24 hours before GTTR injection significantly increased OHC uptake of GTTR in wild-type mice (****$P < 0.0001$; $n \geq 3$) but not in *Trpv1* KO mice (**H**; $n \geq 3$). Error bars, SD. Scale bars, 20 μm.

(Fig. 8B). After chronic treatment with DPBS, $Trpv1^{+/-}$ or *Trpv1* KO mice had negligible differences in basal OHC loss compared to wild-type mice. After chronic LPS-only treatment, $Trpv1^{+/-}$ or *Trpv1* KO mice had marginally less basal OHC loss compared to wild-type mice. Following kanamycin treatment only, wild-type mice generally had increasing OHC loss from the apex basalwards, with negligible OHC loss in $Trpv1^{+/-}$ and *Trpv1* KO mice. In the basal 20% of the cochlea, all three strains had similar degrees of OHC loss after kanamycin-only treatment. However, the number of surviving OHCs (in individual cytocochleogram bins) from upper basal regions of kanamycin-treated cochleae (~16- to 28-kHz region) was significantly fewer in wild-type mice compared to $Trpv1^{+/-}$ or *Trpv1* KO mice [$P < 0.05$, two-way analysis of variance (ANOVA) Tukey's multiple comparisons tests]. After chronic LPS + kanamycin treatment, wild-type mice had substantially greater OHC loss in all cochlear regions (except for the extreme basal 5%) compared to $Trpv1^{+/-}$ or *Trpv1* KO mice (fig. S9 compares treatment groups for each mouse strain). The number of surviving OHCs in individual cytocochleogram bins from a wider region of the basal coil of LPS + kanamycin-treated cochleae (~8- to 32-kHz region) was significantly fewer in wild-type mice compared to $Trpv1^{+/-}$ or *Trpv1* KO mice ($P < 0.05$, two-way ANOVA Tukey's multiple comparisons tests). In toto, our data show that TRPV1 is required to exacerbate kanamycin-induced OHC death during LPS-induced inflammation. Furthermore, extensive OHC survival in heterozygous $Trpv1^{+/-}$ mice compared to wild-type mice following kanamycin treatment (with or without LPS) is suggestive of a dominant negative-like effect in this mutant allele of *Trpv1*.

DISCUSSION

Identifying the molecular mechanisms that facilitate aminoglycoside entry into cochlear sensory hair cells is crucial to develop effective strategies to prevent cochleotoxicity during lifesaving gentamicin

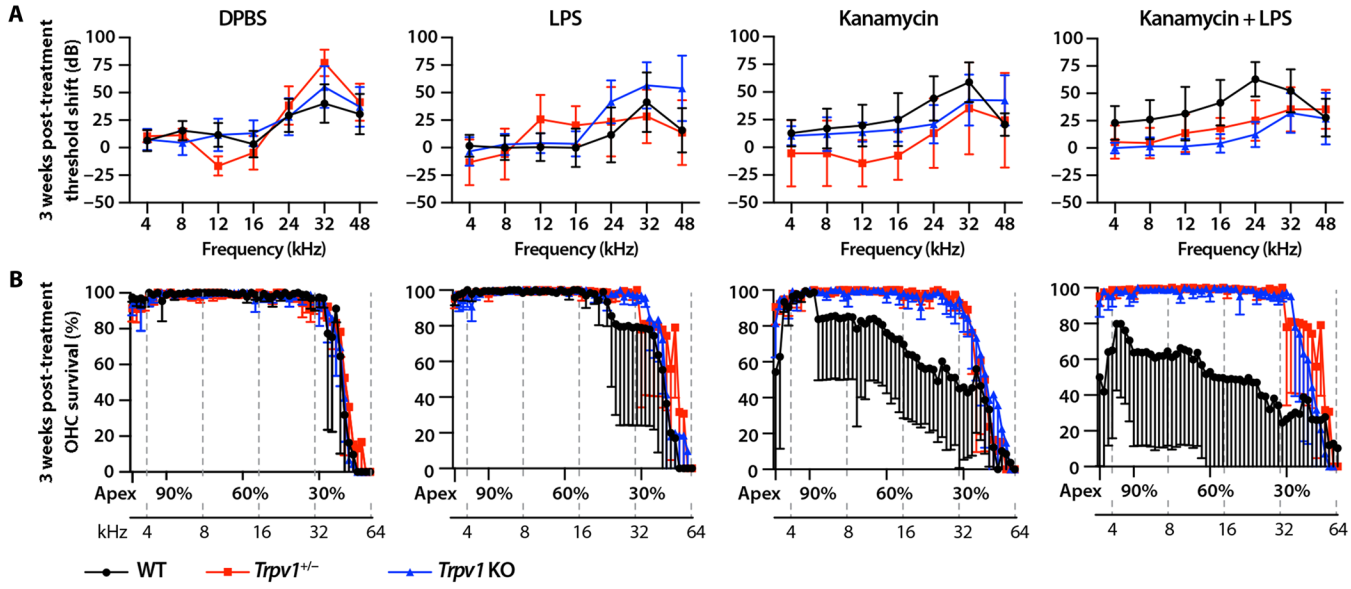

Fig. 8. LPS exacerbates kanamycin-induced hearing loss in wild-type, but not in *Trpv1*$^{+/-}$ or *Trpv1* KO, mice. (**A**) ABR threshold shifts plotted by treatment group at 3 weeks after treatment. Wild-type (WT), *Trpv1*$^{+/-}$, or *Trpv1* KO mice treated with DPBS had similar PTS, except for *Trpv1*$^{+/-}$ mice with significantly improved thresholds at 12 kHz ($P < 0.001$) and larger PTS at 32 kHz ($P < 0.001$). LPS-treated *Trpv1* KO mice had significant PTS compared to wild-type or *Trpv1*$^{+/-}$ mice at 24 and 48 kHz ($P < 0.001$). After kanamycin treatment, wild-type mice generally had greater threshold shifts than *Trpv1* KO mice (except at 48 kHz) and significant threshold shifts compared to *Trpv1*$^{+/-}$ mice at 8, 12, 16, 24, and 32 kHz ($P < 0.05$). Following LPS + kanamycin, wild-type mice had significantly greater threshold shifts ($P < 0.05$) compared to *Trpv1*$^{+/-}$ or *Trpv1* KO mice at all frequencies (except 48 kHz). See tables S4 to S7 for all *P* values; error bars, SD; $n \geq 5$ mice (10 cochleae) per group. (**B**) OHC survival plotted by treatment group at 3 weeks after treatment. Wild-type, *Trpv1*$^{+/-}$, or *Trpv1* KO mice treated with DPBS had negligible OHC losses, except at the extreme basal region of the cochlea, and did not differ from each other. LPS-treated mice also had negligible OHC loss except at the extreme basal 10% region of the cochlea and did not substantially differ from other mouse strains. After kanamycin treatment, wild-type mice generally had greater OHC loss across the majority of the cochlea, except in the apical and extreme basal regions of the cochlea. Following LPS + kanamycin, wild-type mice had greater OHC loss compared to *Trpv1*$^{+/-}$ or *Trpv1* KO mice in all, except the extreme basal regions of the cochlea. $n \geq 5$ mice per group (one cochlea per mouse); error bars, 95% confidence interval derived from two-way ANOVA Tukey's multiple comparisons tests.

pharmacotherapy. Aminoglycosides can enter cells via endocytosis (*9*, *27*), nonselective cation channels including TRP channels and mechanoelectrical transduction channels (*7*, *16*, *23*, *28*), or electrogenic transporters like the sodium glucose transporter-2 (SGLT2) (*17*). Our data here implicate TRPV1 as another channel mediating cellular uptake of aminoglycosides and, crucially, enhanced cochleotoxicity during systemic inflammation.

Agonists of TRPV1 include heat (>43°C), capsaicin, protons (*10*), and other endogenous stimuli (*29*). TRPV1 is expressed throughout the cochlea, and activation by capsaicin elevates auditory thresholds with correspondingly reduced cochlear microphonics and otoacoustic emissions, implicating a regulatory role in cochlear physiology (*12*, *13*). TRPV1 has a pore diameter of ~1 nm (*30*) that can be dilated by agonists (*31*), sufficient to allow permeation by organic molecules like gentamicin with a maximal cross-sectional diameter of ~0.8 nm (*11*). Capsaicin activation of heterologously expressed TRPV1 induced cell death in aminoglycoside-laden culture media (*10*), implicating TRPV1 involvement in aminoglycoside-induced cytotoxicity. Aminoglycosides first enter hair cells before exerting their cytotoxic effect (*2*).

Our in vitro experiments show that TRPV1 agonists increased cellular uptake of (fluorescently tagged) gentamicin and subsequent cytotoxicity. Increasing extracellular [Ca^{2+}] inhibits inward currents mediated by TRPV1 (*10*), decreased cellular uptake of (fluorescently tagged) gentamicin, and ameliorated drug-induced cytotoxicity. Knockdown of endogenous TRPV1 also abrogated gentamicin-induced cytotoxicity. These data are consistent with the hypothesis that gentamicin permeates through TRPV1 channels before exerting cytotoxicity.

Activation of TLR4 can potentiate TRPV1 activity (*25*, *32*), and LPS is a potent TLR4 agonist. In organ of Corti explants from *Pcdh15* KO mice that lack stereociliary tiplinks gating the aminoglycoside-permeant transduction channels (*7*, *8*, *22*), we found that LPS exposure up-regulated expression of TRPV1 in hair cells and marginal cells and enhanced uptake of GTTR. In vivo, systemic LPS also up-regulated TRPV1 expression in marginal cells and hair cells in wild-type mice but not in *Tlr4* KO mice. Systemic LPS also increased cochlear expression of TRPV1 mRNA in wild-type, but not in *Tlr4* KO or *Trpv1* KO, mice. Furthermore, systemic LPS exposure also enhanced OHC uptake of GTTR in wild-type mice but not in *Trpv1* KO mice.

Although TRPV4 and the glucose transporter SGLT2 are also gentamicin permeant, TRPV4 is down-regulated in inner ear ganglia following chronic kanamycin treatment (*33*), while SGLT2 is not normally expressed in the cochlea (*17*). Aminoglycosides are readily taken up by auditory (and vestibular) neurons (*33*, *34*) that could lead to dysfunctional neural activity. Our data here suggest that systemic LPS activates TLR4 to up-regulate cochlear expression of aminoglycoside-permeant TRPV1. This may partially (or wholly) underlie our previous report that systemic LPS-induced inflammation increased cochlear uptake of aminoglycosides and exacerbated subsequent cochleotoxicity (*5*). This interpretation is consistent

with physiological activation of TRPV1 by LPS (and the anti-cancer therapeutic, paclitaxel) in dorsal root ganglia and human embryonic kidney 293 cells (*25*).

TRPV1 also has intracellular physiological roles, and cisplatin treatment up-regulates TRPV1 expression and TRPV1-mediated generation of reactive oxygen species (ROS), driving subsequent cochleotoxicity (*13*, *15*, *20*). Aminoglycosides also induce toxic generation of ROS and subsequent cytotoxicity (*1*). Notably, inhibition of TRPV1 decreases downstream levels of pro-apoptotic signal transducer and activator of transcription-1 (STAT1) relative to pro-survival STAT3 to promote hair cell survival (*20*, *35*). Thus, the improved survival of hair cells and auditory function in mice with mutant *Trpv1* (compared to wild-type mice) during chronic kanamycin (with or without LPS) treatment could also be due to the loss of signaling downstream from TRPV1, as well as reduced TRPV1-mediated aminoglycoside trafficking in the cochlea and uptake by hair cells reported here.

This mutant TRPV1 allele produces a truncated protein product lacking part of the fifth and the entire sixth transmembrane domains that line the channel pore (*36*, *37*). The C-terminal region of this truncated protein in both heterozygous and *Trpv1* KO mice contains the antigen recognized by the TRPV1 antibody used here, as described previously (*38*), and has the same distribution as in wild-type mice (fig. S10). Hence, we used the antigenic peptide as our immunocytochemical control. Multiple studies have validated the lack of TRPV1 functionality using these mutant mice (*39*, *40*). In addition, TRPV1 can be activated (or modulated) by a variety of agonists (or antagonists) that often have nonoverlapping activation (or modulation) sites in the intracellular (Ca^{2+} desensitization), extracellular (protons), or channel pore (capsaicin) domains of TRPV1 (*41*). Thus, our in vivo data may be due to dysfunctional TRPV1 activation/modulation sites independent of the capsaicin-binding site predominantly activated during in vitro studies.

By using *Tlr4* KO mice, we avoided the confounding influence of perturbed protein expression and intracellular activity of TRPV1 in heterozygous and KO *Trpv1* mice. The up-regulation of TRPV1 mRNA and protein expression by LPS in wild-type mice was abolished in *Tlr4* KO mice. Similarly, LPS-enhanced cochlear uptake of gentamicin and cochleotoxicity in wild-type mice was also abrogated in hypofunctional HeJ (*Tlr4*) mice (*5*). These data substantiate the decreased aminoglycoside uptake and subsequent cytotoxicity during exposure to TRPV1 antagonists or siRNA knockdown of TRPV1 in vitro. Thus, we show an apparent correlation between TLR4 activation and up-regulated TRPV1 expression leading to enhanced cochleotoxicity via greater cochlear and hair cell uptake of aminoglycosides and/or signaling downstream of TRPV1. These hypotheses can now be further tested in corresponding preclinical models at key steps along the TLR4 signaling pathway regulating TRPV1 activity (*32*) and subsequent activity downstream of TRPV1, e.g., NOX3 (*13*). It will be important to verify whether the activation of TLR4 that leads to increased TRPV1 expression and activity in OHCs is the same as in other model systems (*25*, *32*). It will also be crucial to determine whether LPS-enhanced GTTR uptake in wild-type OHCs (over and above those from *Pcdh15* KO mice) is indicative of TLR4- or TRPV1-mediated sensitization of TMC1 channels, as for TLR4-mediated sensitization of TRPV1 (*25*). Such sensitization could establish how noise trauma that induces temporary threshold shifts can lead to enhanced GTTR uptake by OHCs (*28*, *42*).

Although cochlear expression of TRPV1 mRNA and protein was up-regulated 24 hours after LPS exposure, increased TRPV1 immunofluorescence could not be detected in spiral ganglion neurons in vivo. This is inconsistent with up-regulated TRPV1 expression in spiral ganglion neurons following chronic kanamycin treatment (*33*). Kitahara *et al.* (*33*) did not observe increased renal expression of TRPV1 following chronic kanamycin treatment. Here, LPS increased renal TRPV1 immunofluorescence (fig. S5), without correspondingly enhanced GTTR uptake, in proximal tubule cells (*5*). This contrast between increased TRPV1 expression without greater GTTR uptake was replicated in supporting cells adjacent to OHCs; yet, OHCs had increased TRPV1 expression and enhanced GTTR fluorescence. These observations further support the hypothesis that agonists can have differential effects on TRPV1 activity and expression in different cell populations, as shown previously for assorted vascular beds (*38*).

The notable preservation of auditory function and hair cell survival following kanamycin treatment (with or without LPS) in heterozygous *Trpv1* (as in *Trpv1* KO) mice is suggestive of a dominant phenotypic effect for this mutant *Trpv1* allele. Only when the tetrameric TRPV1 channel (*37*) contains four wild-type TRPV1 subunits would the channel be functional in these $Trpv1^{+/-}$ mice (a probability of 1/16); otherwise, the channel would be dysfunctional due to the perturbed pore-loop region in one or more participating subunits. Immunolabeling suggests that the truncated TRPV1 subunit could participate in the assembly of nonfunctional channels and localize in similar locations throughout the cell (fig. S10). Assembly of TRPV1 channels is complex and can potentially recruit other TRP subunits, such as TRPV4, resulting in heteromultimerization (*43*, *44*). Nonetheless, channelopathies involving one or more dysfunctional TRPV1 subunits provides one rational explanation for the similarities in audiometric and hair cell survival data from heterozygous and *Trpv1* KO mice during kanamycin ototoxicity (with or without LPS; Fig. 8). Mutations downstream of TLR4, and/or TRPV1, that diminish pro-apoptotic STAT1 levels (*20*, *35*) may underlie the ability of a significant fraction of individuals with cystic fibrosis who maintain typical hearing thresholds despite high cumulative aminoglycoside dosing (*45*). If this interpretation is correct, then attenuating TRPV1 activity during aminoglycoside dosing could effectively ameliorate drug-induced hearing loss, as for cisplatin (*20*, *35*).

CONCLUSION

We show that TRPV1 facilitates cellular uptake of aminoglycosides. Pro-inflammatory signaling via TLR4 enhanced cochlear expression of TRPV1, increasing hair cell uptake of aminoglycosides and subsequent cochleotoxicity that was abolished in heterozygous $Trpv1^{+/-}$ and *Trpv1* KO mice. Thus, TLR4-mediated up-regulation of TRPV1 represents one mechanism that inflammation can enhance aminoglycoside-induced ototoxicity.

MATERIALS AND METHODS

Study design

The objective was to test the hypothesis that TRPV1 expression facilitated cellular uptake of aminoglycosides. We then tested whether LPS-induced inflammation up-regulated cochlear expression of TRPV1 and uptake of GTTR. We then verified that LPS-induced cochlear expression was required to exacerbate aminoglycoside-induced ototoxicity using a well-established protocol for C57BL/6 mice

(*3*). All experiments followed the Animal Research: Reporting of In Vivo Experiments (ARRIVE) reporting guidelines (*46*).

Cell culture and generation of KPT2-Trpv1 cell line

MDCT cells were purchased from the American Type Culture Collection (CRL-3250, Manassas, VA). Mouse kidney proximal tubule (KPT2 and KPT11) and distal tubule (KDT3) cell lines were generated previously (*16*, *17*). Mouse TRPV1 cDNA (Open BioSystems, Lafayette, CO) was amplified by polymerase chain reaction (PCR) using primers 5′-TTT GAA TTC GCC ACC ATG GAG AAA TGG GCT AGC-3′ and 5′-CCC GTC GAC CAT GGA ATC CTT GAA GAC-3′, digested with Eco RI/Sal I, and subcloned into pBabe-puro vector. The resultant plasmid (or empty vector) was transfected into Phoenix-ECO packaging cells using Lipofectamine 2000 (Invitrogen). After 48 hours, the medium containing retrovirus was collected, diluted with growth medium, and added to parental KPT2 cells in culture medium. Culture medium was changed after 24 hours, and puromycin was added in fresh culture medium (2.5 μg/ml) to select for retrovirus-infected cells. From dozens of surviving cells after several days of puromycin treatment, several KPT2-pBabe or KPT2-*Trpv1* clones were selected and expanded as described previously (*16*, *17*) before use for uptake experiments as described below. All cell lines were maintained in Dulbecco's modified Eagle's medium (DMEM) with 10% fetal bovine serum (FBS) at 37°C with 5% CO_2, without streptomycin or penicillin.

Immunoblotting

Immunoblots were performed as previously described (*16*). Briefly, total protein extracts were prepared by homogenizing tissues in lysis buffer with protease inhibitor (Sigma-Aldrich, MO). Proteins in lysis buffer were mixed with SDS sample buffer, resolved in an SDS-polyacrylamide gel, and transferred to polyvinylidene fluoride membrane. After immunoblocking, membranes were incubated overnight with TRPV1 rat polyclonal antibody (cat# ACC-030; Alomone Labs, Jerusalem, Israel) or actin rabbit polyclonal antibody (cat#A2103; Sigma-Aldrich) at 4°C. After incubating with appropriate horseradish peroxidase–conjugated secondary antibodies for 1 hour, chemiluminescence with SuperSignal West Dura Extended Duration Substrate (Thermo Fisher Scientific, Waltham, MA) was used to detect protein expression (*47*).

Immunofluorescence for TRPV1

Cells fixed in 4% paraformaldehyde (PFA) for 20 min at room temperature were washed in DPBS, permeabilized with 0.5% Triton X-100 in DPBS for 30 min, immunoblocked in 10% goat serum in 1% bovine serum albumin (BSA) in PBS for 30 min, and incubated with TRPV1 antisera at 4°C overnight. After washing with immunoblock buffer, cells were incubated with Alexa Fluor 488–conjugated goat anti-rabbit antisera (20 mg/ml) (Invitrogen, Carlsbad, CA) for 60 min, washed, post-fixed with 4% PFA, rinsed, and mounted under coverslips with VectaShield (Vector Labs, CA).

Conjugation and purification of GTTR

Purified GTTR conjugate was produced as previously described (*14*). Briefly, an excess of gentamicin in 0.1 M potassium carbonate solution (pH 10) was mixed with TR succinimidyl esters (Invitrogen, CA) to minimize the possibility of over-labeling individual gentamicin molecules with more than one TR molecule and to preserve the polycationic nature of the conjugate, as previously described. After conjugation, reversed-phase chromatography, using C-18 columns (Grace Division, Discovery Science, IL), was used to purify the conjugate GTTR from unconjugated aminoglycosides and potential contamination by unreacted TR (*27*). The purified GTTR conjugate was aliquoted, lyophilized, and stored desiccated in the dark at −20°C until required.

GTTR uptake studies and confocal microscopy

Cells plated overnight on eight-well chambered coverslips were rinsed with cell medium twice and incubated with GTTR (5 μg/ml) (gentamicin base) in cell culture medium with 1.8 mM Ca^{2+} (#11960–DMEM; Gibco by Life Technologies, Thermo Fisher Scientific, Waltham, MA) for 30 s at room temperature to preclude endocytosis. Cells were rinsed with DPBS three times to remove GTTR from extracellular media before fixation with 4% PFA containing 0.5% Triton X-100 (FATX) for 30 min and washed with DPBS. The cellular distribution of GTTR fluorescence was examined using a Bio-Rad 1024 ES scanning laser system (*5*, *27*). For each individual set of images to be compared, the same confocal settings were used, with two acquisition images per well, two wells per experimental condition, and each experiment performed at least three times to confirm consistency of experimental data. GTTR fluorescent pixel intensities were obtained by the histogram function of the Fiji software after removal of nuclei and intercellular pixels using Adobe Photoshop. Pixel intensities were statistically compared within each set of images per experiment and not compared between different experiments due to varying acquisition settings for replicate experiments to obtain the best dynamic range. To normalize data between experimental sets, the mean intensity was radioed against the control standard and plotted (*17*).

GTTR and gentamicin uptake studies and ELISAs

Cells plated in 60-mm dishes were incubated with GTTR (5 μg/ml), or native gentamicin (1 mM), for 30 s at 37°C, with 5% CO_2. Cells were then homogenized, diluted and centrifuged, and protein was extracted for ELISA. Measurement of total gentamicin levels was determined according to the manufacturer's instructions (EuroProxima, Arnhem, The Netherlands).

TRPV1 agonists and antagonists

Cells plated on chambered coverslips were incubated with GTTR (5 μg/ml) or native gentamicin (1 mM), with or without TRPV1 agonists (3 μM capsaicin, 5 nM RTX, or 0 or 0.16 μM Ca^{2+}) and/or antagonists (0.1 μM I-RTX, 3 or 15 μM capsazepine, or 2 mM Ca^{2+}) for 30 s at 37°C, with 5% CO_2, before fixation for 15 min (*11*). The concentration of 0.16 μM or 2 mM Ca^{2+} was achieved by adding sufficient calcium chloride in 0 mM Ca^{2+} DMEM (#21068—DMEM, no calcium; Gibco by Life Technologies, Thermo Fisher Scientific, Waltham, MA) to reach 0.16 μM or 2 mM Ca^{2+}. Cells were also immunolabeled for TRPV1, or prepared for ELISAs, as described above.

Bactericidal efficacy in the presence of agonists and antagonists

Escherichia coli were grown in Luria-Bertani (LB) broth [1 liter of distilled water, 10 g of tryptone, 5 g of yeast extract, and 10 g of sodium chloride (pH 7.2 ± 0.2)] at 37°C and shaken at 120 rpm for at least 16 hours. Aliquots of fresh LB broth (200 μl) containing *E. coli* (typically 100 μl of LB broth at an optical density of 0.2), gentamicin (4 μg/ml, final concentration), capsaicin (15 μM, final

concentration), capsazepine (15 μM, final concentration), RTX (5 nM, final concentration), I-RTX (100 nM, final concentration), or vehicle were incubated at 37°C for 24 hours in a Tecan Genios Pro plate reader. The optical density was measured hourly at 595 nm, and corresponding growth (kill) curves were constructed.

Cell viability measurements

Cell viability was determined by the reduction of MTT, an indicator of mitochondrial dehydrogenase activity, as previously described (*17*). KPT2, KPT2-pBabe, and KPT2-*Trpv1* cells were plated at 3000 cells per well in a 96-well plate overnight. Cells were treated with gentamicin (5 or 10 mM), with or without capsaicin (3 or 15 μM), or capsazepine (3 or 15 μM) in culture medium for 3 hours. Subsequently, 20 μl of MTT solution (5 mg/ml) was added to each well, and cells were incubated for 4 hours at 37°C, 5% CO_2. Culture medium was then replaced with 200 μl of dimethyl sulfoxide (DMSO) and the optical density was recorded at 540 nm with background subtraction at 660 nm. Cell viability was determined by the reduction of MTT, an indicator of mitochondrial dehydrogenase activity, as previously described (*17*). Student's *t* test was used for statistical analysis (*17*).

TRPV1 siRNA transfection

MDCT cells were plated at 3000 cells per well in an eight-well plate or 60-mm dishes. After overnight incubation to allow cells to attach to the plate or dish, cells were treated with siRNA (Ambion, Thermo Fisher Scientific, MA) for TRPV1 or control siRNA (Invitrogen, CA). Transfection of siRNA was performed using Lipofectamine RNAiMAX (Invitrogen, CA). After 24 hours, transfected cells were fixed and immunoprocessed for TRPV1 immunofluorescence or homogenized for reverse transcription PCR (RT-PCR).

Cochlear coil explants

Colony-founding *Pcdh15*$^{+/-}$ and *Pcdh15* KO mice (*22*, *24*) were purchased from the Jackson Laboratory (stock#: 002072). Four-day-old *Pcdh15*$^{+/-}$ and *Pcdh15* KO pups were anesthetized with ice for 15 min and decapitated. Cochleae were excised and rinsed in cold, sterile PBS, and cochlear coils containing organ of Corti were randomly divided into control or LPS groups. Explants were cultured in DMEM/F12 medium (Invitrogen) containing 10% FBS and ampicillin (0.05 mg/ml) for 24 hours and then treated with culture medium with or without LPS (1 μg/ml) for 1 hour. After washing three times, explants were cultured at 37°C, 5% CO_2 for 24 hours, before incubation with GTTR (1 μg/ml) for 30 min, washing, and 4% PFA fixation as described above. Alternatively, explants were immunoprocessed for TPRV1 immunofluorescence as described above.

In vivo studies

Colony-founding C57BL/6, *Tlr4*$^{-/-}$, *Trpv1*$^{+/-}$, or *Trpv1* KO mice were obtained from the Jackson Laboratory [stock#: 007227 (*Tlr4* KO) or 003770 (*Trpv1* KO)]. Mice (15 to 25 g, 4 to 8 weeks old) were randomly assigned into control (DPBS) or experimental (LPS) groups. Mice received a tail vein injection of DPBS (50 μl/10 g) or LPS (1 mg/kg), followed by an intraperitoneal injection of GTTR (2 mg/kg) 24 hours later. One hour after GTTR injection, mice were cardiac-perfused with DPBS, followed by 4% PFA in DPBS. Cochleae or renal tissues were then excised and immersion-fixed in 4% PFA (*5*). Fixed tissues were permeabilized with 0.5% Triton X-100 for 45 min, washed, processed for TRPV1 immunofluorescence as described above, washed and counter-labeled with Alexa Fluor 488–conjugated phalloidin, post-fixed for 15 min, and washed. Organ of Corti tissues were mounted under coverslips with VectaShield and imaged using a Bio-Rad MRC 1024 ES laser scanning confocal system attached to a Nikon Eclipse TE300 inverted microscope (*5*). Additional wild-type, *Trpv1*$^{+/-}$, *Trpv1* KO, or *TLR4* KO mice treated with DPBS or LPS, administered GTTR (2 mg/kg) as appropriate, were fixed 24 hours later before processing for TRPV1 immunofluorescence by confocal microscopy as needed.

For serum and cochlear ELISAs, C57, *Trpv1*$^{+/-}$, and *Trpv KO* mice received a tail vein injection of DPBS or LPS, followed by an intraperitoneal injection of gentamicin (20 μg/g) 24 hours later, as described above. One or 3 hours after gentamicin injection, cardiac blood samples were obtained before cardiac perfusion with DPBS followed by 4% PFA, and cochleae were excised and frozen at −20°C. Serum and homogenized cochleae were diluted and centrifuged, and protein was extracted as needed for ELISA. Total gentamicin levels in serum and cochlear tissues were determined according to the manufacturer's instructions (EuroProxima, Arnhem, The Netherlands).

PCR and mRNA studies

C57BL/6 J, *Trpv1*$^{-/-}$, and *Tlr4*$^{-/-}$ mice were randomly grouped and treated with LPS or DPBS for 24 hours. After perfusion with DPBS, excised cochlea samples were placed in RNAlater (Ambion) and stored at −80°C. Tissue RNA was extracted from homogenization of whole cochlea, quantified by absorbance at 260 nm, normalized, reverse-transcribed using an RT^2 first strand kit (QIAGEN), and prepared for RT-PCR using custom PCR arrays optimized for reaction conditions, *Trpv1* primer (Bio-Rad), and *GAPDH* (glyceraldehyde-3-phosphate dehydrogenase) primer (QIAGEN). Each sample was run and analyzed in triplicate, and the Ct values for *Trpv1* were subtracted from the Ct values of *GAPDH* to yield ΔCt values. The average ΔCt was calculated for the control group, and this value was subtracted from the ΔCt of all other samples (including the control group). This resulted in a ΔΔCt value for all samples, which was then used to calculate the fold induction of the mRNA levels of *Trpv1* using the formula $2^{-\Delta\Delta Ct}$.

Auditory brainstem responses

ABRs to pure tones were used to ensure normal cochlear function before toxicity studies and determine threshold shifts following kanamycin treatment (*17*). Briefly, needle electrodes were placed subcutaneously below the test ear, at the vertex, with a ground electrode near the paw. Each ear of each anesthetized mouse was stimulated individually with a closed tube sound delivery system sealed into the ear canal. The ABR to 1-ms rise-time tone burst stimuli at 4, 8, 12, 16, 24, 32, and 48 kHz was recorded, and thresholds were obtained for each ear. Only mice with normal bilateral, baseline ABR thresholds were used.

Ototoxicity studies

For toxicity studies, C57BL/6 (wild type), *Trpv1*$^{+/-}$, or *Trpv1* KO mice (4 to 6 weeks old) were randomly divided into four groups per strain: (i) DPBS only, (ii) LPS only, (iii) kanamycin only, and (iv) LPS plus kanamycin. Mice received kanamycin (850 mg/kg) (or an equal volume of DPBS) twice daily subcutaneously for 15 consecutive days (*3*). Mice received a tail vein injection of LPS (1 mg/kg) [or DPBS (50 μl/10 g)] the day before kanamycin treatment and on the 5th and 10th day during kanamycin treatment (*5*). ABRs were obtained before kanamycin treatment and 1 and 21 days after kanamycin

treatment before cardiac perfusion and fixation as described above, followed by processing for Alexa Fluor 488 phalloidin and Hoechst nuclear labeling, followed by whole-mounting of cochlear coils for confocal imaging with an Olympus FV1000 confocal microscope for hair cell apices and nuclei. Naïve operators blinded to treatment groups constructed cytocochleograms counting the presence or absence of hair cells along the length of the cochlea in ImageJ software (*3*, *5*). The frequency map and the length of each cochlea were obtained using the Measure Line and MosaicJ plugins in the ImageJ software.

Statistical analyses

Statistical analyses were chosen on the basis of data under analysis. In brief, Student's unpaired *t* test was used for GTTR or TRPV1 fluorescence intensity analyses, as well as for gentamicin or GTTR ELISA studies. For ABR analyses, we used two-way ANOVA with Tukey's post hoc tests. The statistical analyses used, number of replicate measurements, or mice are stated in each figure legend, and P values <0.05 were considered significant. A two-way ANOVA using Bonferroni post hoc multiple comparison test correction was used for cytocochleograms to test for differences between groups.

SUPPLEMENTARY MATERIALS

Supplementary material for this article is available at http://advances.sciencemag.org/cgi/content/full/5/7/eaaw1836/DC1

Fig. S1. Stable heterologous expression of TRPV1 in selected cell lines.
Fig. S2. RTX-enhanced TRPV1-mediated uptake of gentamicin is attenuated by extracellular [Ca^{2+}].
Fig. S3. Viability of cell lines incubated with a TRPV1 agonist or antagonist.
Fig. S4. Agonists and antagonists of TRPV1 do not affect the bactericidal efficacy of aminoglycosides.
Fig. S5. LPS enhanced TRPV1 expression in renal cells in vivo.
Fig. S6. LPS did not enhance strial uptake of GTTR in *Trpv1* KO mice in vivo.
Fig. S7. LPS exacerbates kanamycin-induced hearing loss in wild-type, but not in *Trpv1*$^{+/-}$ or *Trpv1* KO, mice.
Fig. S8. LPS increases cochlear (but not serum) levels of gentamicin.
Fig. S9. LPS exacerbates kanamycin-induced OHC loss in wild-type, but not in *Trpv1*$^{+/-}$ or *Trpv1* KO, mice.
Fig. S10. TRPV1 immunolabeling in cochlear tissues from wild-type and *Trpv1* KO mice.
Table S1. Significant differences in threshold at 3 weeks after treatment from baseline for wild-type (C57) mice.
Table S2. Significant differences in threshold at 3 weeks after treatment from baseline for *Trpv1*$^{+/-}$ mice.
Table S3. Significant differences in threshold at 3 weeks after treatment from baseline for *Trpv1* KO mice.
Table S4. Significant differences in thresholds between strains at 3 weeks after treatment with DPBS only.
Table S5. Significant differences in thresholds between strains at 3 weeks after treatment with LPS only.
Table S6. Significant differences in thresholds between strains at 3 weeks after treatment with kanamycin only.
Table S7. Significant differences in thresholds between strains at 3 weeks after treatment with LPS + kanamycin.
Table S8. Significant differences in thresholds between treatment groups at 3 weeks after treatment for wild-type (C57) mice.
Table S9. Significant differences in thresholds between treatment groups at 3 weeks after treatment for *Trpv1*$^{+/-}$ mice.
Table S10. Significant differences in thresholds between treatment groups at 3 weeks after treatment for *Trpv1* KO mice.

REFERENCES AND NOTES

1. A. Forge, J. Schacht, Aminoglycoside antibiotics. *Audiol. Neurootol.* **5**, 3–22 (2000).
2. H. Hiel, J.-P. Erre, C. Aurousseau, R. Bouali, D. Dulon, J.-M. Aran, Gentamicin uptake by cochlear hair cells precedes hearing impairment during chronic treatment. *Audiology* **32**, 78–87 (1993).
3. W.-J. Wu, S.-H. Sha, J. D. McLaren, K. Kawamoto, Y. Raphael, J. Schacht, Aminoglycoside ototoxicity in adult CBA, C57BL and BALB mice and the Sprague-Dawley rat. *Hear. Res.* **158**, 165–178 (2001).
4. P. E. Mohr, J. J. Feldman, J. L. Dunbar, A. McConkey-Robbins, J. K. Niparko, R. K. Rittenhouse, M. W. Skinner, The societal costs of severe to profound hearing loss in the United States. *Int. J. Technol. Assess. Health Care* **16**, 1120–1135 (2000).
5. J.-W. Koo, L. Quintanilla-Dieck, M. Jiang, J. Liu, Z. D. Urdang, J. J. Allensworth, C. P. Cross, H. Li, P. S. Steyger, Endotoxemia-mediated inflammation potentiates aminoglycoside-induced ototoxicity. *Sci. Transl. Med.* **7**, 298ra118 (2015).
6. C. P. Cross, S. Liao, Z. D. Urdang, P. Srikanth, A. C. Garinis, P. S. Steyger, Effect of sepsis and systemic inflammatory response syndrome on neonatal hearing screening outcomes following gentamicin exposure. *Int. J. Pediatr. Otorhinolaryngol.* **79**, 1915–1919 (2015).
7. W. Marcotti, S. M. van Netten, C. J. Kros, The aminoglycoside antibiotic dihydrostreptomycin rapidly enters mouse outer hair cells through the mechano-electrical transducer channels. *J. Physiol.* **567**, 505–521 (2005).
8. B. Pan, N. Akyuz, X.-P. Liu, Y. Asai, C. Nist-Lund, K. Kurima, B. H. Derfler, B. György, W. Limapichat, S. Walujkar, L. N. Wimalasena, M. Sotomayor, D. P. Corey, J. R. Holt, TMC1 forms the pore of mechanosensory transduction channels in vertebrate inner ear hair cells. *Neuron* **99**, 736–753.E6 (2018).
9. E. Hashino, M. Shero, R. J. Salvi, Lysosomal augmentation during aminoglycoside uptake in cochlear hair cells. *Brain Res.* **887**, 90–97 (2000).
10. M. J. Caterina, M. A. Schumacher, M. Tominaga, T. A. Rosen, J. D. Levine, D. Julius, The capsaicin receptor: A heat-activated ion channel in the pain pathway. *Nature* **389**, 816–824 (1997).
11. S. E. Myrdal, P. S. Steyger, TRPV1 regulators mediate gentamicin penetration of cultured kidney cells. *Hear. Res.* **204**, 170–182 (2005).
12. J. Zheng, C. Dai, P. S. Steyger, Y. Kim, Z. Vass, T. Ren, A. L. Nuttall, Vanilloid receptors in hearing: Altered cochlear sensitivity by vanilloids and expression of TRPV1 in the organ of Corti. *J. Neurophysiol.* **90**, 444–455 (2003).
13. D. Mukherjea, S. Jajoo, K. Sheehan, T. Kaur, S. Sheth, J. Bunch, C. Perro, L. P. Rybak, V. Ramkumar, NOX3 NADPH oxidase couples transient receptor potential vanilloid 1 to signal transducer and activator of transcription 1-mediated inflammation and hearing loss. *Antioxid. Redox Signal.* **14**, 999–1010 (2011).
14. H. Li, P. S. Steyger, Systemic aminoglycosides are trafficked via endolymph into cochlear hair cells. *Sci. Rep.* **1**, 159 (2011).
15. T. Kaur, D. Mukherjea, K. Sheehan, S. Jajoo, L. P. Rybak, V. Ramkumar, Short interfering RNA against STAT1 attenuates cisplatin-induced ototoxicity in the rat by suppressing inflammation. *Cell Death Dis.* **2**, e180 (2011).
16. T. Karasawa, Q. Wang, Y. Fu, D. M. Cohen, P. S. Steyger, TRPV4 enhances the cellular uptake of aminoglycoside antibiotics. *J. Cell Sci.* **121**, 2871–2879 (2008).
17. M. Jiang, Q. Wang, T. Karasawa, J.-W. Koo, H. Li, P. S. Steyger, Sodium-glucose transporter-2 (SGLT2; SLC5A2) enhances cellular uptake of aminoglycosides. *PLOS ONE* **9**, e108941 (2014).
18. D. N. Furness, C. M. Hackney, P. S. Steyger, Organization of microtubules in cochlear hair cells. *J. Electron Microsc. Tech.* **15**, 261–279 (1990).
19. P. S. Steyger, D. N. Furness, C. M. Hackney, G. P. Richardson, Tubulin and microtubules in cochlear hair cells: Comparative immunocytochemistry and ultrastructure. *Hear. Res.* **42**, 1–16 (1989).
20. D. Mukherjea, S. Jajoo, C. Whitworth, J. R. Bunch, J. G. Turner, L. P. Rybak, V. Ramkumar, Short interfering RNA against transient receptor potential vanilloid 1 attenuates cisplatin-induced hearing loss in the rat. *J. Neurosci.* **28**, 13056–13065 (2008).
21. G. P. Richardson, I. J. Russell, Cochlear cultures as a model system for studying aminoglycoside induced ototoxicity. *Hear. Res.* **53**, 293–311 (1991).
22. K. N. Alagramam, R. J. Goodyear, R. Geng, D. N. Furness, A. F. J. van Aken, W. Marcotti, C. J. Kros, G. P. Richardson, Mutations in protocadherin 15 and cadherin 23 affect tip links and mechanotransduction in mammalian sensory hair cells. *PLOS ONE* **6**, e19183 (2011).
23. A. Alharazneh, L. Luk, M. Huth, A. Monfared, P. S. Steyger, A. G. Cheng, A. J. Ricci, Functional hair cell mechanotransducer channels are required for aminoglycoside ototoxicity. *PLOS ONE* **6**, e22347 (2011).
24. K. N. Alagramam, C. L. Murcia, H. Y. Kwon, K. S. Pawlowski, C. G. Wright, R. P. Woychik, The mouse Ames waltzer hearing-loss mutant is caused by mutation of *Pcdh15*, a novel protocadherin gene. *Nat. Genet.* **27**, 99–102 (2001).
25. Y. Li, P. Adamek, H. Zhang, C. E. Tatsui, L. D. Rhines, P. Mrozkova, Q. Li, A. K. Kosturakis, R. M. Cassidy, D. S. Harrison, J. P. Cata, K. Sapire, H. Zhang, R. M. Kennamer-Chapman, A. B. Jawad, A. Ghetti, J. Yan, J. Palecek, P. M. Dougherty, The cancer chemotherapeutic paclitaxel increases human and rodent sensory neuron responses to TRPV1 by activation of TLR4. *J. Neurosci.* **35**, 13487–13500 (2015).
26. J. F. Willott, Changes in frequency representation in the auditory system of mice with age-related hearing impairment. *Brain Res.* **309**, 159–162 (1984).
27. S. E. Myrdal, K. C. Johnson, P. S. Steyger, Cytoplasmic and intra-nuclear binding of gentamicin does not require endocytosis. *Hear. Res.* **204**, 156–169 (2005).
28. R. S. Stepanyan, A. A. Indzhykulian, A. C. Vélez-Ortega, E. T. Boger, P. S. Steyger, T. B. Friedman, G. I. Frolenkov, TRPA1-mediated accumulation of aminoglycosides in mouse cochlear outer hair cells. *J. Assoc. Res. Otolaryngol.* **12**, 729–740 (2011).

29. E. Cao, J. F. Cordero-Morales, B. Liu, F. Qin, D. Julius, TRPV1 channels are intrinsically heat sensitive and negatively regulated by phosphoinositide lipids. *Neuron* **77**, 667–679 (2013).
30. A. Jara-Oseguera, I. Llorente, T. Rosenbaum, L. D. Islas, Properties of the inner pore region of TRPV1 channels revealed by block with quaternary ammoniums. *J. Gen. Physiol.* **132**, 547–562 (2008).
31. D. Bautista, D. Julius, Fire in the hole: Pore dilation of the capsaicin receptor TRPV1. *Nat. Neurosci.* **11**, 528–529 (2008).
32. J.-J. Lin, Y. du, W.-K. Cai, R. Kuang, T. Chang, Z. Zhang, Y.-X. Yang, C. Sun, Z.-Y. Li, F. Kuang, Toll-like receptor 4 signaling in neurons of trigeminal ganglion contributes to nociception induced by acute pulpitis in rats. *Sci. Rep.* **5**, 12549 (2015).
33. T. Kitahara, H.-S. Li, C. D. Balaban, Changes in transient receptor potential cation channel superfamily V (TRPV) mRNA expression in the mouse inner ear ganglia after kanamycin challenge. *Hear. Res.* **201**, 132–144 (2005).
34. Y.-B. Zhang, R. Zhang, W.-F. Zhang, P. S. Steyger, C.-F. Dai, Uptake of gentamicin by vestibular efferent neurons and superior olivary complex after transtympanic administration in guinea pigs. *Hear. Res.* **283**, 169–179 (2012).
35. V. Borse, R. F. H. Al Aameri, K. Sheehan, S. Sheth, T. Kaur, D. Mukherjea, S. Tupal, M. Lowy, S. Ghosh, A. Dhukhwa, P. Bhatta, L. P. Rybak, V. Ramkumar, Epigallocatechin-3-gallate, a prototypic chemopreventative agent for protection against cisplatin-based ototoxicity. *Cell Death Dis.* **8**, e2921 (2017).
36. M. J. Caterina, A. Leffler, A. B. Malmberg, W. J. Martin, J. Trafton, K. R. Petersen-Zeitz, M. Koltzenburg, A. I. Basbaum, D. Julius, Impaired nociception and pain sensation in mice lacking the capsaicin receptor. *Science* **288**, 306–313 (2000).
37. M. Liao, E. Cao, D. Julius, Y. Cheng, Structure of the TRPV1 ion channel determined by electron cryo-microscopy. *Nature* **504**, 107–112 (2013).
38. C. A. Sand, A. D. Grant, M. Nandi, Vascular expression of transient receptor potential vanilloid 1 (TRPV1). *J. Histochem. Cytochem.* **63**, 449–453 (2015).
39. H. E. Gibson, J. G. Edwards, R. S. Page, M. J. Van Hook, J. A. Kauer, TRPV1 channels mediate long-term depression at synapses on hippocampal interneurons. *Neuron* **57**, 746–759 (2008).
40. J. M. Rosen, R. E. Yaggie, P. J. Woida, R. J. Miller, A. J. Schaeffer, D. J. Klumpp, TRPV1 and the MCP-1/CCR2 axis modulate post-UTI chronic pain. *Sci. Rep.* **8**, 7188 (2018).
41. L. Ma, F. Yang, S. Vu, J. Zheng, Exploring functional roles of TRPV1 intracellular domains with unstructured peptide-insertion screening. *Sci. Rep.* **6**, 33827 (2016).
42. H. Li, A. Kachelmeier, D. N. Furness, P. S. Steyger, Local mechanisms for loud sound-enhanced aminoglycoside entry into outer hair cells. *Front. Cell. Neurosci.* **9**, 130 (2015).
43. M. J. M. Fischer, J. M. Edwardson, V_2A_2lidating TRP channel heteromers. *Temperature* **1**, 26–27 (2014).
44. N. Hellwig, N. Albrecht, C. Harteneck, G. Schultz, M. Schaefer, Homo- and heteromeric assembly of TRPV channel subunits. *J. Cell Sci.* **118**, 917–928 (2005).
45. G. Al-Malky, R. Suri, S. J. Dawson, T. Sirimanna, D. Kemp, Aminoglycoside antibiotics cochleotoxicity in paediatric cystic fibrosis (CF) patients: A study using extended high-frequency audiometry and distortion product otoacoustic emissions. *Int. J. Audiol.* **50**, 112–122 (2011).
46. C. Kilkenny, W. J. Browne, I. C. Cuthill, M. Emerson, D. G. Altman, Improving bioscience research reporting: The ARRIVE guidelines for reporting animal research. *PLOS Biol.* **8**, e1000412 (2010).
47. M.-Y. Jiang, J. Chen, J. Wang, F. Xiao, H.-H. Zhang, C.-R. Zhang, D.-S. Du, Y.-X. Cao, L.-L. Shen, D.-N. Zhu, Nitric oxide modulates cardiovascular function in the rat by activating adenosine A_{2A} receptors and inhibiting acetylcholine release in the rostral ventrolateral medulla. *Clin. Exp. Pharmacol. Physiol.* **38**, 380–386 (2011).

Acknowledgments: The illustrations were drafted by K. Thiebes, Simplified Science Publishing LLC. We acknowledge R. Larisch and the OHRC Mouse Core for colony management. **Funding:** This work was supported by NIH-NIDCD grants R01 DC004555, R01 DC012588, and P30 DC005983 (to P.S.S.) and by DoD W81XWH-14-1-0006 (to H.L.). Funding agencies had no role in study design, data collection and analysis, manuscript preparation manuscript, or decision to publish. **Ethics statement:** The care and use of all mice in this study were approved by the Institutional Animal Care and Use Committee of Oregon Health & Science University (IACUC approval #IS00001801). **Author contributions:** M.J., H.L., and P.S.S. conceived and designed the experiments; M.J., A.J., T.K., F.T., Y.Z., W.B.M., and P.S.S. performed the experiments and analyzed the data; M.J., A.K., and P.S.S. contributed reagents/materials/analysis tools; M.J., H.L., and P.S.S. wrote and edited the manuscript; and M.J., A.J., T.K., F.T., Y.Z., W.B.M., H.L., and P.S.S. revised and approved the manuscript. **Competing interests:** The authors declare that they have no competing interests. **Data and materials availability:** All data needed to evaluate the conclusions in the paper are present in the paper and/or the Supplementary Materials. Additional data related to this paper may be requested from the authors. Purified GTTR conjugate can be provided by P.S.S. pending scientific review and a completed material transfer agreement. Requests for purified GTTR should be submitted to petersteyger@creighton.edu.

Submitted 26 November 2018
Accepted 13 June 2019
Published 17 July 2019
10.1126/sciadv.aaw1836

Citation: M. Jiang, H. Li, A. Johnson, T. Karasawa, Y. Zhang, W. B. Meier, F. Taghizadeh, A. Kachelmeier, P. S. Steyger, Inflammation up-regulates cochlear expression of TRPV1 to potentiate drug-induced hearing loss. *Sci. Adv.* **5**, eaaw1836 (2019).

Science Advances

Inflammation up-regulates cochlear expression of TRPV1 to potentiate drug-induced hearing loss

Meiyan Jiang, Hongzhe Li, Anastasiya Johnson, Takatoshi Karasawa, Yuan Zhang, William B. Meier, Farshid Taghizadeh, Allan Kachelmeier and Peter S. Steyger

Sci Adv **5** (7), eaaw1836.
DOI: 10.1126/sciadv.aaw1836